PHYSICAL REVIEW A **76**, 010101(R) (2007)

Classical-quantum correspondence in electron-positron pair creation

N. I. Chott, Q. Su, and R. Grobe
Intense Laser Physics Theory Unit and Department of Physics, Illinois State University, Normal, Illinois 61790-4560, USA
(Received 9 October 2006; published 18 July 2007)

We examine the creation of electron-positron pairs in a very strong force field. Using numerical solutions to quantum field theory we calculate the spatial and momentum probability distributions for the created particles. A comparison with classical mechanical phase space calculations suggests that despite the fully relativistic and quantum mechanical nature of the matter creation process, most aspects can be reproduced accurately in terms of classical mechanics.

DOI: 10.1103/PhysRevA.76.010101 PACS number(s): 12.20.Ds, 03.70.+k, 11.10.−z

As a conceptually simpler and computationally more feasible theoretical framework, classical mechanics can sometimes provide valuable insight into the dynamics of linear and nonlinear quantum mechanical systems [1,2]. Quite remarkably, classical mechanics can even provide an adequate description for systems that require *quantum field theory*. In fact, we will suggest that several features of the creation process of matter from vacuum can be recovered with astonishing accuracy by simple classical mechanical calculations. More specifically, we compute the spatial and momentum probability distributions of electron-positron pairs that are created in a very strong force field using quantum field theory with spatial and temporal resolution.

The electron-positron field operator $\Psi(t)$ can be computed from numerical solutions to the time-dependent Dirac equation, $i\partial\Psi(t)/\partial t=h(t)\Psi(t)$, where the spatial representation of the Dirac-Hamiltonian (in atomic units) is given by $h(t)=c\alpha p+\beta c^2+V(z,t)$, where α and β denote the 4×4 Pauli matrices and c (=137.036 a.u.) is the speed of light. Details of the CPU intensive computations on a space-time lattice can be found in Refs. [3,4]. The specific form of the force field is not so important; for our analysis we use the potential $V(z,t)=V_0\ [(1-\tanh(z/W))/2]\ \Gamma(t)$, whose gradient represents a spatially localized force field along the z direction [5] that is turned on via $\Gamma(t)=\sin^2[\pi t/(2T)]$ for $0<t<T$ and $\Gamma(t)=1$ for $t>T$ with $T=5.1\times10^{-6}$ a.u. The potential height V_0 was chosen as $2c^2-10^4$ a.u., which is less than twice the rest mass energy of the electron such that pairs can be created in the region $-W<z<W$ from vacuum not due to supercriticality induced spontaneous emission but because of the time dependence of the force field [6]. For a recent generalization of the Schwinger formula for the pair-production probability in a time-dependent supercritical field, see [7].

In contrast to the S-matrix based in or out formalism that can predict asymptotic observables, we need to predict all stages of the pair creation process with full temporal and spatial resolution. It has been pointed out [6] that the interaction zone *inside* a space- and time-dependent force is theoretically difficult to access. Physical properties of real particles inside the interaction zone cannot be obtained directly from the usual (time-independent) fermionic annihilation or creation operators that are associated with (asymptotic) free particle states [8]. In this work, however, we propose a method to compute all observables for the electron *inside* the interaction region. In this approach, the electronic portion of the quantum field operator, denoted by $\Psi_e(t)$, has to be computed. This can be achieved by projecting the full electron-positron field $\Psi(t)$ onto the submanifold of the Hilbert space of instantaneous energy eigenstates $|p_{(t)}\rangle$ with energies $e_{p(t)}$ larger than $-c^2$, defined as $h(t)|p_{(t)}\rangle=e_{p(t)}|p_{(t)}\rangle$. It is important to note that these instantaneous states $|p_{(t)}\rangle$ are not time-evolved states. The electronic part of the field operator, obtained as $\Psi_e(t)\equiv\Sigma_p|p_{(t)}\rangle\langle p_{(t)}|\Psi(t)$, is a generalization of the so-called positive frequency part of Ψ, discussed in textbooks [9] for the special case of time-independent systems. $\Psi_e(t)$ is the key quantity to determine the electronic properties. As an example, the electrons' density operator $\rho(t)$ can be computed through the (Fock-space) expectation value with the initial multiparticle state, the field-free vacuum $\|\text{vac}\rangle$, according to $\rho(t)=\langle\text{vac}\|\Psi_e^\dagger(t)\Psi_e(t)\|\text{vac}\rangle$. The diagonal elements of this 4×4 operator $\rho(t)$ in its spatial and momentum representations determine the spatial and momentum probability distributions, $P(z,t)\equiv\langle z|\rho(t)|z\rangle$ and $P(k,t)\equiv\langle k|\rho(t)|k\rangle$, respectively.

The sequence of graphs in Fig. 1 shows (with the solid lines) snapshots of $P(z,t)$ and $P(k,t)$ at five times t. To set the spatial scale, the dashed line next to the position dependent graphs [Figs. 1(a), 1(c), and 1(e)] shows the extent of the potential $V(z)$. The dynamics is characterized by three temporal regimes, the creation domain $(0<t<5.1\times10^{-6}$ a.u.) during which the force is turned on, is characterized by a nearly shape-invariant growth of both densities, $P(z,t)=P_0(z)f(t)$ and $P(k,t)=P_0(k)f(t)$. The subscript in $P_0(\ldots)$ denotes the shape-invariant birth density and $f(t)$ is the total yield. This creation stage is followed by the acceleration out of the (repulsive) force region [Figs. 1(c) and 1(d)] and finally the force-free evolution [Figs. 1(e) and 1(f)]. The latter snapshots for $t=2.9\times10^{-3}$ a.u. show that most electrons are accelerated by the force into the positive z direction corresponding to a positive momentum. Some of the electrons, however, escape to $z<0$, reflecting those electrons (called errants [10]) that were able to escape opposite to the direction of the very force that created them. While the electrons' spatial density keeps spreading as the particles escape with various energies, the momentum density reaches its asymptotic distribution once the particles have left the interaction region. This particular density is experimentally most accessible as detectors are typically located outside the interaction region and measure the energy spectrum related to $P(k,t)$.

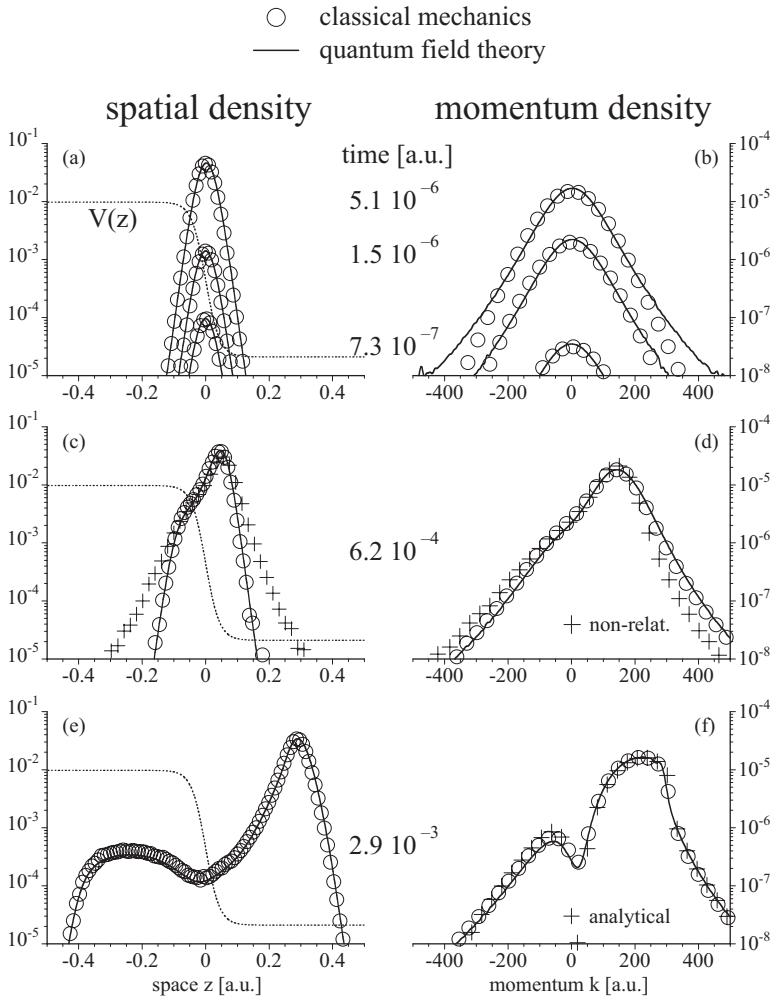

FIG. 1. Comparison of quantum field theory (solid lines) with classical mechanics (open circles). The snapshots of the spatial (left column) and momentum (right column) distributions $P(z,t)$ and $P(k,t)$ of the electrons created from vacuum in a strong force field. The dashed line in the left column is the potential $V(z)$ (on a linear scale) responsible for the pair creation. The crosses in (c) and (d) represent nonrelativistic calculations. In (f) the crosses represent an analytical formula [Eq. (2)] for the asymptotic momentum spectrum. The total norm of the classical mechanical data were normalized to match the quantum field theoretical yields. [$V_0 = 2c^2$-10^4 a.u., $W=6/c$, classical data are obtained from 1.5×10^6 orbits.]

In order to compare the spatial and momentum distributions with those computed from classical mechanics, we have to know the functional form of the birth phase space density $P_{\mathrm{cl}}(z,k)$. If the field theoretical densities based on the transition matrix elements of $V(z)$ are expanded perturbatively for short times, one can find under certain nonrelativistic approximations to the energy eigenstates remarkably simple analytical forms for the birth densities for an arbitrary potential $V(z)$, $P_0(z) \approx |dV(z)/dz|^2$ and $P_0(k) \approx |dV(kW/c)/dk|^2$. These intuitive and universal expressions agree nicely with the QFT data [circles in Figs. 1(a) and 1(b)] and show, e.g., that the spatial birth density $P_0(z)$ is directly proportional to the square of the force field. Deviations are expected for forces $V'(z)$ that are spatially more localized than the Compton wavelength of the electron, $1/c$, and also for longer turn on times for which the time scales for creation and subsequent acceleration by the force are no longer separable. In this domain the spatial regions would contain a mixture of particles that were accelerated and that were just created at that location [11].

Quantum field theory does not necessarily give us immediate information about the correlation between the initial momentum k and position z, so as a first step we just *assume* that the classical phase space density $P_{\mathrm{cl}}(z,k)$ is initially given by the (uncorrelated) product of the corresponding marginal densities, $P_{\mathrm{cl}}(z,p)=P_0(z)P_0(k)$. The validity of this hypothesis will be examined in Fig. 2 below. The time evolution of the phase space density can be obtained as the solution to the Liouville equation for the Hamilton function $h_{\mathrm{cl}} \equiv \sqrt{[c^4+c^2k^2]}+V(z)$,

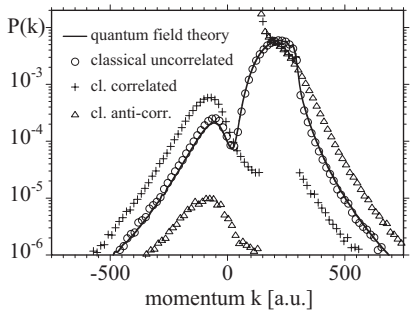

FIG. 2. The impact of the momentum-position correlation in the birth phase space density $P_0(z,k)$. The quantum field theoretical momentum distribution $P(k,t)$ at time $t=2.9\times10^{-3}$ a.u. (solid line) is compared with predictions for classical ensembles with various degrees of correlation, no correlation (open circles), maximum correlation (crosses), and anticorrelation (triangles) (same parameters as in Fig. 1).

$$P_{\mathrm{cl}}(z,k,t) = \int\int dz_0 dk_0 P_{\mathrm{cl}}(z_0,k_0)\,\delta[z - z_{\mathrm{cl}}(z_0,k_0,t)] \times \delta[k - k_{\mathrm{cl}}(z_0,k_0,t)], \quad (1)$$

where z_{cl} and k_{cl} denote classical particle orbits with initial conditions $z_{\mathrm{cl}}(z_0,k_0,t=0)=z_0$ and $k_{\mathrm{cl}}(z_0,k_0,t=0)=k_0$. They can be obtained as numerical solutions to the Hamilton equations, $dz/dt=dh_{\mathrm{cl}}/dk$ and $dk/dt=-dh_{\mathrm{cl}}/dz$.

The open circles in Fig. 1 show the predictions for the marginal densities, obtained via $P_{\mathrm{cl}}(z,t)\equiv\int dk\, P_{\mathrm{cl}}(z,k,t)$ and $P_{\mathrm{cl}}(k,t)\equiv\int dz\, P_{\mathrm{cl}}(z,k,t)$. The agreement with the quantum field theoretical data is nearly perfect for all times. Even though the prediction of the total yield requires quantum field theory and the overall norm of $P_{\mathrm{cl}}(z,t)$ and $P_{\mathrm{cl}}(k,t)$ were matched, it is remarkable that nearly all details of the momentum as well as spatial distributions are quite accurately reproduced by classical mechanics for each of the three stages of the dynamics.

As mentioned above, we are particularly interested in computing the asymptotic momentum density, $P_\infty(k)\equiv\int dz\, P(z,k,t\to\infty)$. It can be derived fully analytically and does not require any solution to the Hamilton equations. It is made up of three contributions, $P_\infty(k)=\int dz_0\,[F_1(z_0)+F_2(z_0)+F_3(z_0)]$, with

$$F_1(z_0) \equiv P(z_0,\tilde{k}_L)\sqrt{\{k^2(c^4+c^2\tilde{k}_L{}^2)/[\tilde{k}_L{}^2(c^4+c^2k^2)]\}}\,\theta[-k],$$

$$F_2(z_0) \equiv P(z_0,-\tilde{k}_R)\sqrt{\{k^2(c^4+c^2\tilde{k}_R{}^2)/[\tilde{k}_R{}^2(c^4+c^2k^2)]\}}\,\theta[-\tilde{k}_R - k_{\min}(z_0)]\theta[k-k^*(z_0)],$$

$$F_3(z_0) \equiv P(z_0,\tilde{k}_R)\sqrt{\{k^2(c^4+c^2\tilde{k}_R{}^2)/[\tilde{k}_R{}^2(c^4+c^2k^2)]\}}\,\theta[k - k^*(z_0)]. \quad (2)$$

We have used several abbreviations, the unit-step function $\theta(z)\equiv(|z|+z)/|2z|$, the maximum initial momentum to overcome the potential barrier $k_{\min}(z_0)\equiv -\sqrt{\{[c^2+V_0-V(z_0)]^2-c^4\}}/c$, the lower bound for the initial momentum to escape to the right $k^*(z_0)\equiv\sqrt{[V(z_0)^2+2V(z_0)c^2]}/c$, and $\tilde{k}_L(z_0,k)\equiv -\sqrt{\{[\sqrt{(c^4+c^2k^2)}+V_0-V(z_0)]^2-c^4\}}/c$ and $\tilde{k}_R(z_0,k)\equiv\sqrt{\{[\sqrt{(c^4+c^2k^2)}-V(z_0)]^2-c^4\}}/c$. As the three functions F_1, F_2, and F_3 in Eq. (2) can be directly associated with electrons ejected to $z<0$ (errants) and electrons with birth momenta $k_0<0$ and $k_0>0$ that are accelerated into the positive z direction, this solution permits a microscopic insight into the importance of the pre- and postacceleration dynamics for the final energy distribution.

Having established this excellent classical-quantum field theoretical correspondence permits us to use classical mechanics instead of the more difficult QFT to obtain some first insight into three rather fundamental questions, concerning the importance of relativity, initial state correlation, and the dynamical relevance of interparticle forces.

In order to examine the importance of a relativistic treatment, we have repeated the classical simulations for a nonrelativistic time evolution, which can be obtained in the limit of the parameter $c\to\infty$. Due unrestricted velocities, the nonrelativistic spatial density (crosses) in Fig. 1(c) is much wider than its relativistic counterpart (circles and solid line). If the (canonical) momentum density in Fig. 1(d) were graphed as a function of the velocity $kc^2/\sqrt{(c^4+c^2k^2)}$, the strict upper limit $P(k)=0$ for velocities $>c$ would be apparent for the QFT calculation.

Second, the quantum-classical agreement seems to suggest that the position and momentum in the (exact) quantum density $P_0(z,k)$ at birth might be rather uncorrelated. In order to probe a possible impact of correlations, we have repeated the classical mechanical simulation for an initial phase space density with the same marginal densities as above, however, with highly correlated position and momentum variables, $P_{\mathrm{cl}}(z,k)\equiv P_0(z)\ P_0(k)\ \delta(z\text{-}kW/c)$. In this case the electrons' positions depend on their momentum, large positions are associated with large momenta. In the opposite case of anticorrelated variables, $P_{\mathrm{cl}}(z,k)\equiv P_0(z)\ P_0(k)\ \delta(z+kW/c)$, electrons with large momenta are located at small z. In Fig. 2 we show that these two types of correlations can lead to drastically different final momentum densities, suggesting that in the true QFT process the location and momentum are rather independent variables at birth; of course, more systematic studies could clarify further details.

Third, the quantum field description based on the Dirac equation did not include interfermionic interactions (based on an exchange of photons), such as the electron-positron attraction. To account for this interaction in quantum field theory would require the inclusion of the vector potential as a dynamically coupled second-quantized field operator, but any solution to the combined Dirac-Maxwell operator equations is presently far beyond computational feasibility. The classical mechanical simulations, however, are simple enough such that this interaction can be included at least phenomenologically and a first insight into its impact can be obtained. For short distances, this force is not known, but a comparison of the functional forms of lowest-order terms of the quantum field theoretical transition amplitudes and nonrelativistic transition matrix elements [8,12] suggests that for large inter-particle separations the potential is Coulombic, $\sim 1/|z_e\text{-}z_p|$, where z_e and z_p are the electron and positron positions. We have therefore examined a set of long-range forces that are asymptotically Coulombic, of the functional form $\sim 1/\sqrt{[(z_e\text{-}z_p)^2+s^2]}$, where the parameter s represents an unknown screening length.

In Fig. 3 we display the classical mechanical momentum distribution $P(k,t)$ for $t=2.9\times10^{-3}$ a.u. obtained for three screening lengths, $s=10^{-3}$, 10^{-4}, and 10^{-5} a.u. The comparison with the QFT data (solid line) suggests that as long as any (true) screening parameter is larger than $s=10^{-3}$ a.u., the resulting effect of the electron-positron attraction is negligible compared to the interaction with the external force. The small size of $s=10^{-3}$ a.u. also suggests that only those few particles that are closer to each other [13] than a hundredth of the Compton wavelength ($1/c=7.3\times10^{-3}$ a.u.), can be affected by the mutual force. The linear vertical scale of the quantum data $P(k,t)$ in Fig. 3 reveals also small oscillatory and time-dependent contributions for 200 a.u. $<k<$ 280 a.u.

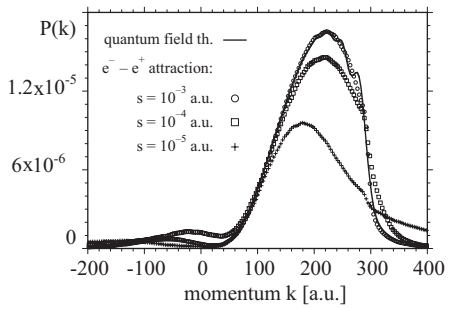

FIG. 3. The impact of the Coulomb force between the electrons and positrons. The quantum field theoretical momentum distribution $P(k,t)$ at time $t=2.9\times10^{-3}$ a.u. (solid line) is compared with predictions for classical ensembles with three degrees of screening. Note the oscillatory behavior in $P(k,t)$ for 200 a.u. $<k<$ 280 a.u. associated with quantum interferences cannot be matched with classical mechanics (same parameters as in Fig. 1).

that are reminiscent of quantum interferences and obviously cannot be predicted from a classical phase space density.

In summary, we have shown how quantum field theory can be used to analyze the creation dynamics of particles inside a spatially and temporally dependent force field. This was possible by projecting the field operator on a set of instantaneous energy eigenstates with energies above the negative energy threshold. We computed the spatial and momentum densities of the created electron-positron pairs and showed that the quantum field theoretical data can be reproduced with remarkable accuracy by means of classical phase space calculations. As classical mechanical ensemble computations are much more efficient than quantum field theoretical approaches, they open the field to several new challenges that were previously technically inaccessible. Future studies might examine three-dimensional aspects including temporal, spatial, and spectral properties of possible laser pulses, possible ponderomotive force effects [14], the impact of possible nuclei, any interparticle Coulombic forces and many other challenges. The microscopic insight obtained and its first qualitative answers will be of relevance in the near future, as laser sources are predicted to become available [15–17] that are powerful enough to create electron-positron pairs from vacuum and therefore open ways to control the pair-creation dynamics.

We acknowledge many discussions with I. Bialynicki-Birula, S. Bowen, and C.C. Gerry. This work has been supported by the NSF. We also acknowledge support from the Research Corporation for Cottrell Science Awards, and NCSA for supercomputing time.

[1] M. C. Gutzwiller, *Chaos in Classical and Quantum Mechanics* (Springer-Verlag, New York, 1990).
[2] F. Haake, *Quantum Signatures of Chaos* (Springer, Berlin, 1991).
[3] J. W. Braun, Q. Su, and R. Grobe, Phys. Rev. A **59**, 604 (1999).
[4] P. Krekora, Q. Su, and R. Grobe, Phys. Rev. Lett. **92**, 040406 (2004).
[5] F. Sauter, Z. Phys. **69**, 742 (1931); **73**, 547 (1931).
[6] W. Greiner, B. Müller, and J. Rafelski, *Quantum Electrodynamics of Strong Fields* (Springer-Verlag, Berlin, 1985).
[7] F. Cooper and G. C. Nayak, see e-print arXiv:hep-th/0612292.
[8] M. E. Peskin and D. V. Schroeder, *An Introduction to Quantum Field Theory* (Westview, New York, 1995).
[9] See, e.g., S. S. Schweber, *An Introduction to Relativistic Quantum Field Theory* (Harper & Row, New York, 1962).
[10] P. Krekora, K. Cooley, Q. Su, and R. Grobe, Laser Phys. **16**, 588 (2006).
[11] C. C. Gerry, Q. Su, and R. Grobe, Phys. Rev. A **74**, 044103 (2006).
[12] R. H. Landau, *Quantum Mechanics II* (Wiley, New York, 1990).
[13] P. Krekora, Q. Su, and R. Grobe, Phys. Rev. Lett. **93**, 043004 (2004).
[14] R. R. Freeman, T. J. McIlrath, P. H. Bucksbaum, and M. Bashkansky, Phys. Rev. Lett. **57**, 3156 (1986).
[15] G. A. Mourou, T. Tajima, and S. V. Bulanov, Rev. Mod. Phys. **78**, 309 (2006).
[16] C. D. Roberts, S. M. Schmidt, and D. V. Vinnik, Phys. Rev. Lett. **89**, 153901 (2002).
[17] D. B. Blaschke, A. V. Prozorkevich, C. D. Roberts, S. M. Schmidt, and S. A. Smolyansky, Phys. Rev. Lett. **96**, 140402 (2006).